

Nuclear properties at finite temperature in a two-component statistical model

P. Bhattacharyya,¹ S. Das Gupta,^{1,2} and A. Z. Mekjian¹

¹*Department of Physics and Astronomy, Rutgers University, Piscataway, New Jersey 08855-0849*

²*Physics Department, McGill University, 3600 University Street, Montréal, Québec, Canada H3A 2T8*

(Received 7 April 1999; published 18 October 1999)

An exactly solvable model is developed for multifragmentation which is an extension of an earlier model, to two-component systems. The model is quite versatile. One can use experimental binding energies and excited states of clusters as inputs to the model and compute, rather easily, many observables. In this paper we pay particular attention to specific heats (hence the caloric curves) of certain target projectile combinations. In idealized cases without Coulomb interactions, large systems show signatures of a first order phase transition. The caloric curves change significantly when Coulomb energy is included. [S0556-2813(99)02411-5]

PACS number(s): 25.70.Pq, 24.10.Pa, 64.60.My

I. INTRODUCTION

Several experimental [1–5] and theoretical [6–12] investigations into heavy-ion collisions at intermediate to high energies have indicated the presence of a liquid-gas-like phase transition in nuclear matter. There is however much debate [13,14] on whether or not this phase transition disappears when isospin degrees of freedom are included, i.e. when protons and neutrons are distinguished in the models. To answer this question satisfactorily one needs to study these two-component models elaborately.

However, this poses difficulties. Two-component models are generally computationally much more intensive than one-component models. As a result, it is harder to look at large two-component systems. In this paper we study a class of two-component models which overcomes these difficulties. The models are computationally tractable so that calculations on a few hundred particles is possible. The models are also parametrically flexible, admitting a wide range of behaviors for certain model-independent features to be studied. We used binding energies from experiments as inputs and this, in our opinion, makes the calculations quite realistic and allows theoretical predictions to be compared directly with experiments. The attractive feature of the model is that only modest computing power is needed and the results obtained are exact.

When the excitation energy per nucleon in a collision is of the order of the binding energy of the nucleon, the stability of the nucleus is threatened. More importantly, the shell structure of the nucleus becomes meaningless and the nucleus behaves as a continuous mass of nucleons which are basically indistinguishable from each other on all counts except charge. The nucleus gets hotter during the collision and expands. This expansion causes internal fractures in the nucleus and eventually the nucleus splits into various other nuclei [6]. The end of this expansion process is called “freeze-out” and at this point, the volume of the nucleus is sufficiently large for nuclear interactions between different fragments to become negligible. Hence the nuclear fragment composition does not change after “freeze-out.”

The formation of various nuclear fragments from the original composite nucleus is called an event. The occurrence of a specific event is dictated by the conditions of the collision. The nuclear interactions leading to this particular

event can be very complicated and a dynamic description of the process is therefore very difficult. However, the number of possible events is so large that such a dynamic calculation may not be necessary. Instead, a statistical treatment, which will analyze the probability of an event can be employed to give good results. Hence, we will set up a statistical model to describe the situation.

II. A GENERIC TWO-COMPONENT MODEL

In this section, we describe a very general model for two-component systems. This model can be used for any system consisting of two kinds of objects, z of the first kind and n of the second kind. The z objects and n objects are distinguishable from each other but not amongst themselves. The general model describes clustering in such a system. There are several ways in which, clustering can occur. Each way is called a partition of the z and n objects that make up the system. This is equivalent to bipartite partitioning [15,16] of integers, i.e., partitioning two integers simultaneously. Let each partition be denoted by a “vector” \vec{n} , where the components of \vec{n} , n_{jk} are labeled by two free indices, one for the number of objects of the first kind, and one for the second kind, such that $\vec{n} = (n_{01}, n_{10}, n_{02}, n_{11}, n_{20}, \dots)$, where n_{jk} counts the number of clusters with j objects of the first kind and k of the second. Clearly then, \vec{n} has to satisfy the following two constraints:

$$\sum_{jk} j n_{jk} = z, \quad (1)$$

$$\sum_{jk} k n_{jk} = n. \quad (2)$$

The probability for a particular partition can be calculated as follows. Let x_{jk} be the one particle partition function of the jk cluster. (A jk cluster has j objects of the first kind and k of the second.) If we assume that the various clusters do not interact, the statistical weight for a particular \vec{n} [$W(\vec{n})$] should be the product of the one-particle partition functions of all the jk clusters. But taking into account the fact that all jk clusters are indistinguishable,

$$W(\vec{n}) = \prod_{j=0}^z \prod_{k=0}^n \frac{x_{jk}^{n_{jk}}}{n_{jk}!}, \quad (3)$$

where the $n_{jk}!$ term introduces a Gibbs' reduction in the phase space volume amongst the jk clusters. The partition function for the system can then be given by summing the weights of all the possible partitions, i.e.,

$$Z_{zn} = \sum_{\vec{n}} W(\vec{n}). \quad (4)$$

Therefore, once x_{jk} is specified, the partition function can be calculated. This is facilitated by the fact that the expectation value of the number of jk clusters is given by

$$\langle n_{jk} \rangle = \frac{x_{jk}}{Z_{zn}} \frac{\partial Z_{zn}}{\partial x_{jk}} \quad (5)$$

$$= \frac{x_{jk}}{Z_{zn}} Z_{z-j, n-k}. \quad (6)$$

Using Eq. (6) in Eq. (1) gives

$$Z_{zn} = \frac{1}{z} \sum_{jk} j x_{jk} Z_{z-j, n-k}. \quad (7)$$

From this, the partition function can be calculated recursively starting with $Z_{00} = 1$. [A similar expression can also be obtained from Eq. (2).]

The basic physics of the above model is the same as in most statistical models. The assumption is that the phase space is the sole criterion. Given this premise one can use the microcanonical ensemble [19] which conserves baryon number, charge number, and energy exactly or use the model here which conserves baryon number, charge number but uses a constant temperature rather than constant energy thereby allowing a fluctuation in energy. The advantage in our approach is the ease with which calculations can be done for realistic cases. Also noteworthy is the fact that all partitions (there are millions of them) are included: no Monte Carlo is needed to generate these partitions. The model is quite different from BUU [1] or QMD [29] types of models. The last ones do not assume equilibrium, rather they are transport type models. The difficulty there is that for practical purposes, the calculations are either classical or semiclassical. While there are certainly questions that transport models can answer but equilibrium models cannot, for calculations of yields of composites the lack of quantum mechanics imposes severe limitations on currently available transport models. All shell effects are lost and the properties of composites are far removed from reality. Besides, computation of yields in these types of models are much more computer intensive.

III. CHOICE OF x_{jk}

The application of the above model to nuclear systems is obvious. The two kinds of objects are protons and neutrons and a partition is nothing but an event in a collision. A jk

cluster now refers to a nucleus with j protons and k neutrons. The physics of the situation therefore, lies in x_{jk} . We will do all our calculations in the canonical ensemble. So we assume that at freeze-out, the nucleons participating in the collision occupy a volume V_n and are in equilibrium at a temperature T .

x_{jk} is thus, the partition function of a nucleus with j protons and k neutrons. Quite generally this is given by $x_{jk} = [V(2\pi mT)^{3/2}(j+k)^{3/2}/h^3] \sum_i \exp[-\beta E_{jk}(i)]$, where V is the available volume to the participating nucleons. The first part in x_{jk} is due to the kinetic energy of the center of mass of the cluster as obtained from integrating over all the possible momenta of all the clusters. The second part is the internal partition function of the jk cluster and it is a sum over all the energy levels of an isolated jk cluster.

The versatility of the model lies in the many choices of x_{jk} that can be made through different choices of E_{jk} . Values can be taken from experiment or from suitable parametrization. The limitation of the model is that interaction between different clusters cannot be included except through a one body mean field approximation. Therefore we use a Wigner-Seitz approximation to include the effects of the long range Coulomb field.

Properties of this model where no distinction is made between neutrons and protons were studied in Ref. [17]. Further studies can be found in Ref. [28].

IV. THERMODYNAMICS

From the partition function, the various thermodynamic variables of interest, such as the free energy, the specific heat at constant volume and the average expectation value of the size of the largest nucleus can be determined. The free energy (F) is of interest as its first derivative will show a break in the event of a first-order phase transition. F is calculated from

$$F = -\frac{1}{\beta} \ln(Z_{zn}), \quad (8)$$

where β is the inverse temperature.

The specific heat (c_V) per nucleon should show a peak that scales with the size of the system. It is calculated from

$$\frac{c_V}{k_B} = \left(\frac{\partial U}{\partial T} \right)_V, \quad (9)$$

where U is the internal energy and is given by

$$U = -\frac{\partial \ln(Z_{zn})}{\partial \beta} = \frac{T^2}{Z_{zn}} \sum_{jk} Z_{z-j, n-k} \frac{\partial x_{jk}}{\partial T}. \quad (10)$$

In deriving the above equation we used Eq. (3) and Eq. (4) of the previous section. It can be shown that Eq. (10) reduces to a more transparent form given by

$$U = \sum \langle n_{jk} \rangle U_{jk}, \quad (11)$$

where U_{jk} is the average energy of a jk cluster.

The average expectation value of the size of the largest nucleus ($\langle a_{\max} \rangle / A$) is of interest because it can play the role of the order parameter in our system. For each event possible, the largest nucleus is labeled a_{\max} and $\langle a_{\max} \rangle$ is calculated over all possible configurations as follows. If any x_{jk} is set to zero, by virtue of Eq. (6), $\langle n_{jk} \rangle$ is also zero. Therefore that jk cluster is no longer allowed. So the probability of a being the largest nucleus is proportional to

$$Z_{zn}(x_1, x_2, \dots, x_a, 0, \dots) - Z_{zn}(x_1, x_2, \dots, x_{a-1}, 0, \dots),$$

where x_a is a shorthand notation referring to all the jk clusters with $j+k=a$. The first term will allow clusters of size 1 to a to be the largest clusters and the second, those of size 1 to $a-1$. Therefore, the difference gives the weight of distributions with a as the largest nucleus. Summing these weights over all the possible a 's gives the normalization factor.

V. AN IDEAL CASE

Before studying a realistic case by incorporating the various energy terms for each jk cluster, it is instructive to do parametric calculations as these bring out several interesting points. By switching off the Coulomb term one can study the nuclear matter limit and many studies of phase transitions in this limit exist. In this limit we find close correspondence with the idealized one-component model that was the predecessor to this study [17]. We then incorporate the Coulomb term and find that there are significant changes to the caloric curve.

We approximate the ground state energy of the jk cluster using the mass-energy formula, i.e., $E_{g.s.} = a_v(j+k) - a_s(j+k)^{2/3} - b_s(j-k)^2/(j+k)$. The first term is the volume energy contribution. A value of 16 MeV was used for a_v . The second term is the surface term. The surface area is proportional to $(j+k)^{2/3}$ and $a_s = 18$ MeV is the surface coefficient. The b_s term gets bigger when the difference between the numbers of protons and neutrons in a cluster gets bigger. The negative sign of the term ensures the suppression of this effect.

Excitation energies of the nuclei can be incorporated using a low temperature expansion of the Fermi-gas model. This yields a multiplicative factor $\exp[T(j+k)/\epsilon_0]$, where $\epsilon_0 = 4\epsilon_F/\pi^2 = 16$ MeV. It has been argued that this factor, monotonic in T , should reach an asymptotic limit. Hence following Ref. [19], we introduce a cutoff factor to achieve this effect.

Therefore, incorporating the various energy levels in the jk cluster, we obtain

$$x_{jk} = \frac{V}{h^3} (2\pi mT)^{3/2} (j+k)^{3/2} \exp\left(\frac{a_v(j+k)}{T} - \frac{a_s(j+k)^{2/3}}{T} - \frac{b_s(j-k)^2}{T(j+k)} + \frac{TT_0(j+k)}{\epsilon_0(T+T_0)}\right). \quad (12)$$

$x_{jk} = V(2\pi mT)^{3/2}/h^3$ when $j+k=1$.

Here T_0 is taken to be 12 MeV and $V = 2.2V_0$. V_0 is normal nuclear volume V , as defined previously, is the avail-

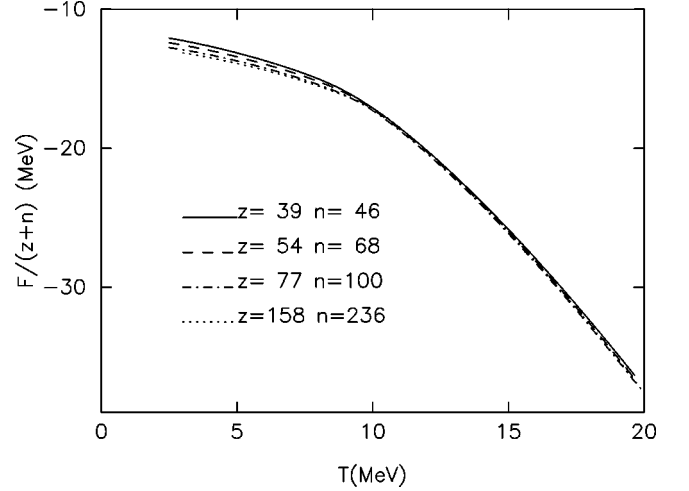


FIG. 1. Free energy per nucleon in a model with no Coulomb effects. The binding energy is approximated by the liquid drop formula. Excited states are accounted for by a modified Fermi-gas expression. There appears to be a break in the first derivative of $F/(z+n)$. For very large systems this break is much more pronounced.

able free volume given by $V = V_n - V_{\text{ex}}$ where V_{ex} is the excluded volume due to the finite sizes of the clusters. The details of the excluded volume are complicated [18] but V_{ex} is often approximated to be a constant. Its value is needed in estimating the Coulomb interaction in the Wigner-Seitz approximation and we use the Hahn-Stöcker value [20] of $V_{\text{ex}} = V_0$.

VI. ROLE OF SURFACE TERM

In this work we choose to show results for four (z, n) combinations: these are (39,46), (54,68), (77,100), and (158,236). They were chosen to represent some typical target-projectile combinations, the lowest being Sc+Ar and the highest Au+Au. The magnitude of the slope of the free energy per particle for all of these (Fig. 1) is much smaller below 9 MeV than above 10 MeV. For one kind of particle and for very large systems an abrupt break in the first derivative was established in Ref. [17] leading to an unambiguous signature of a first order phase transition. Very large systems in the two-component model have not been studied yet so that we cannot yet claim that it is the remnant of a first order transition as will be reflected in finite systems. We do find that there is a peak in the specific heat between 9 and 10 MeV indicating a phase transition.

Figure 2 is a plot of $Y(j)$ against j where $Y(j) = \sum_k \langle n_{jk} \rangle$, is proportional to the yield of the isotope of charge j . Below the temperature (T_B) at which the phase transition occurs, the yield $Y(j)$ falls with j , reaches a minimum, rises, reaches a maximum after which it falls off very quickly. Above T_B , the yield $Y(j)$ decreases monotonically with j . The disappearance of the maximum at high j can be regarded as the signal of the phase change.

The specific heat per nucleon (Fig. 3) shows a strong peak which scales with the size of the system. This occurs at the

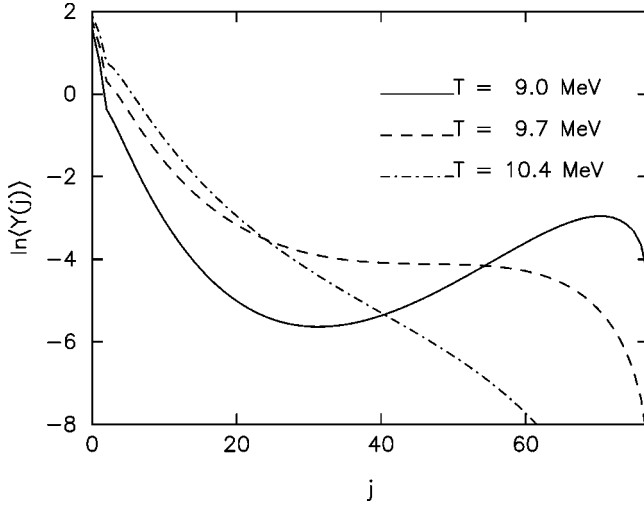


FIG. 2. Average yields of different isotopes at various temperatures in the same model as in Fig. 1.

same temperature as the break in the free energy, again a strong indicator of a phase transition. c_V can be shown to be

$$c_V = \frac{3}{2} \sum_{jk} \langle n_{jk} \rangle + \frac{2(z+n)}{\epsilon_0} \frac{TT_0^3}{(T+T_0)^3} + \sum_{jk} \frac{\partial \langle n_{jk} \rangle}{\partial T} \left(\frac{3}{2}T + a_s(j+k)^{2/3} + b_s \frac{(j-k)^2}{(j+k)} \right). \quad (13)$$

The various contributions to c_V are analyzed separately in Fig. 4. The first term in Eq. (13) is the translational term (since $\sum_{jk} \langle n_{jk} \rangle$ is the total number of clusters) and it increases sharply around the transition temperature and saturates. The second term is due to excitations and it drops off with T . Of the others, $\sum_{jk} \langle \partial \langle n_{jk} \rangle / \partial T \rangle T$ shows a very small

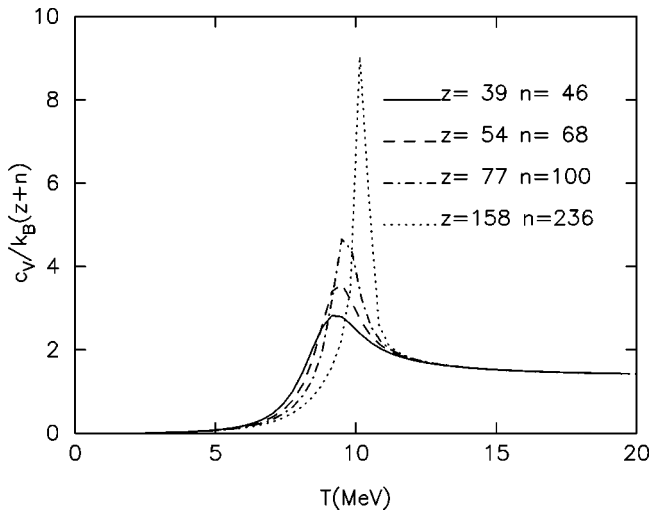


FIG. 3. Specific heat per nucleon for the model in Fig. 1. The peak in specific heat becomes higher and narrower as the size of the system increases. In the thermodynamic limit, the peak is a δ function. The Coulomb effect changes this result.

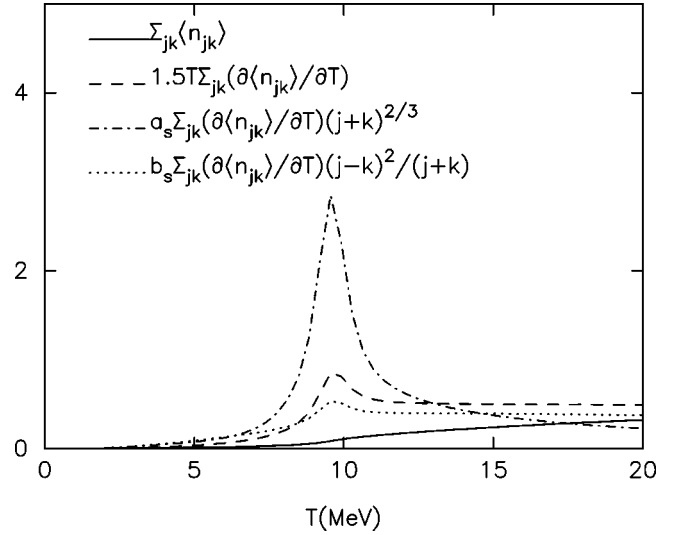


FIG. 4. Various contributions to the specific heat per nucleon of Fig. 3 for $z=77$, $n=100$. The most dominant term is the surface term. The text gives more details.

bump as does $\sum_{jk} \langle \partial \langle n_{jk} \rangle / \partial T \rangle b_s (j-k)^2 / (j+k)$. In the absence of the surface term, these small peaks are washed out by the translational term. So the only interesting term is $\sum_{jk} \langle \partial \langle n_{jk} \rangle / \partial T \rangle a_s (j+k)^{2/3}$. This shows the peak that appears in c_V . This can be explained based on the fact that the infinite cluster no longer exists for $T > T_B$. At T_B , $\langle \partial \langle n_{jk} \rangle / \partial T \rangle$ is nonzero for this cluster and $(j+k)^{2/3}$ is appreciable (since $j+k \approx z+n$) and the product is therefore, very large. Hence, a large peak is seen at T_B . From this, we can conclude that the surface term is entirely responsible for the phase transition. Indeed the sharpness of $\sum \langle \partial \langle n_{jk} \rangle / \partial T \rangle$ is also due to the surface term.

$\langle a_{\max} \rangle$ was calculated and it shows a sharp drop at the ‘‘boiling point’’ (Fig. 5). The larger the system, the sharper is the drop. The case of very large system can be seen in Ref. [17]. In the thermodynamic limit, this is due to the disap-

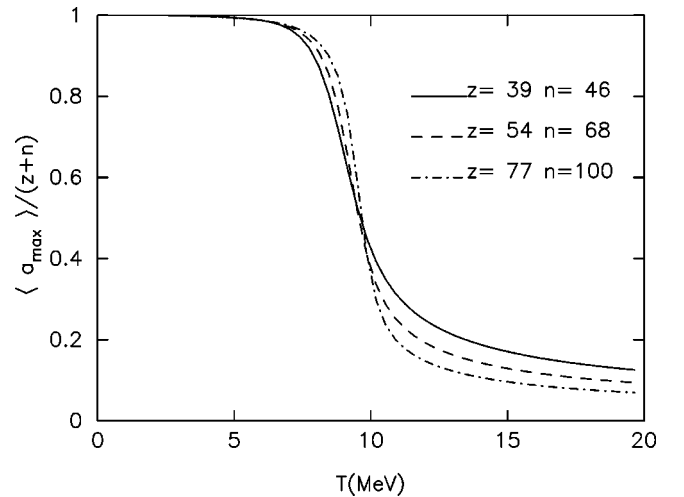


FIG. 5. Average value of the size of the largest cluster divided by the total number of nucleons in the same model as in the earlier figures. The bigger the system, the sharper the drop.

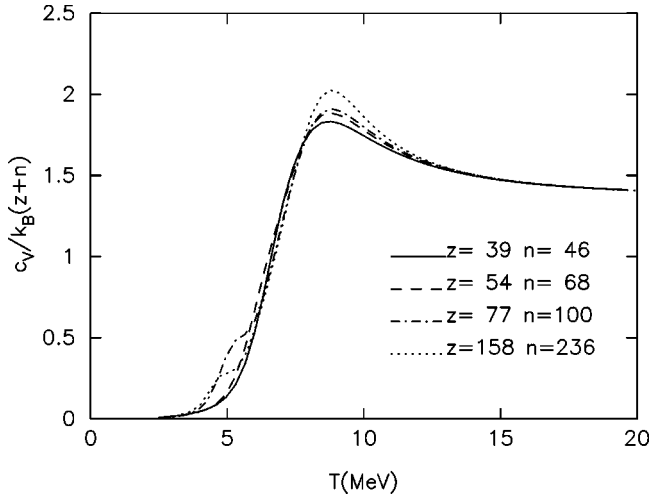


FIG. 6. Specific heat per nucleon using a parametrized mass formula with Coulomb interaction included via the Wigner-Seitz approximation. Of significance is the fact that the peak in specific heat per nucleon is now more or less independent of the size of the system.

pearance of the infinite cluster. At $T < T_B$, the size of the largest cluster is of the order of $z+n$ and so $\langle a_{\max} \rangle / (z+n)$ is finite. But at $T > T_B$, only smaller clusters exist and $\langle a_{\max} \rangle / (z+n)$ is very small.

VII. APPROXIMATE INCLUSION OF COULOMB INTERACTION

We now add to this parametric version of binding energy the effect of the Coulomb interaction via the Wigner-Seitz approximation. Apart from an inconsequential term which does not change at constant volume and is also independent of temperature, incorporation of Wigner-Seitz approximation modifies the thermodynamics of the system by adding to the internal energy of each composite of charge je and radius R a term given by $[3(je)^2/5R][1 - (V_0/V_n)^{1/3}]$ where V_0/V_n is the ratio of normal nuclear volume to the volume at the time of dissociation. We have taken this ratio to be 1/3.2.

The Coulomb term has a significant effect on c_V . Without Coulomb, the specific heat per particle becomes larger at the boiling point for a larger system (it approaches a delta function in the thermodynamic limit) but Coulomb interaction inhibits this growth leading to a c_V per particle that is much less dependent on the size of the system (Fig. 6). This means that the caloric curve is approximately independent of the specific target-projectile combination used. This feature remains unchanged in the more realistic case considered in the next section.

VIII. CALCULATION WITH EXPERIMENTAL BINDING ENERGIES

We now report studies of a calculation in which the ground state binding energies are read from data tables, i.e., x_{jk} is now given by

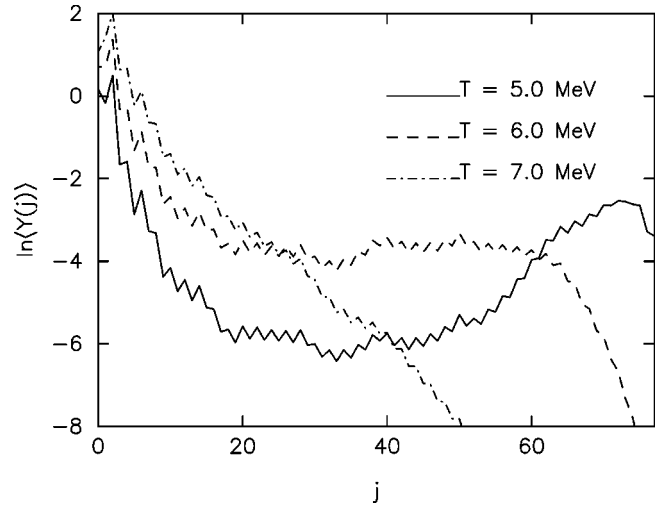


FIG. 7. For this and the two following figures, the binding energies of the clusters are taken from experimental data and the Coulomb interaction between clusters is included through the Wigner-Seitz approximation. The yields of isotopes are shown at three different temperatures for $z=77$, $n=100$. The characteristics are the similar to those in Fig. 2 but shell structure effects are clearly visible.

$$x_{jk} = \frac{V}{h^3} (2\pi mT)^{3/2} (j+k)^{3/2} \exp \left[\frac{a_{V_{jk}}}{T} + \frac{TT_0}{\epsilon_0(T+T_0)} (j+k) + \frac{3}{5R} \frac{(je)^2}{T} \left(\frac{V}{V_n} \right)^{1/3} \right], \quad (14)$$

where $a_{V_{jk}}$ is the binding energy of the jk cluster from Ref. [21]. $a_{V_{jk}}$ therefore encompasses all the terms (volume, surface, and Coulomb self-energy terms) of the previous model. When a jk cluster does not exist x_{jk} is set to zero. Coulomb interaction between clusters is incorporated via the Wigner-Seitz approximation. Since experimental binding energies are used shell-effects are included.

Figure 7 shows the isotopic yield $Y(j)$ against j at different temperatures. The general characteristics of Fig. 2 can still be seen but now there are interesting structures because of shell effects and the odd-even effects are clearly discernible. At high temperature (not shown here) the shell effects disappear and a smooth curve results. Unfortunately one still cannot compare the isotope yields at this stage to experimental data because the yields shown here are at finite temperatures and contain populations of both particle stable and particle unstable states. To compute the yield of a given nucleus two more calculations are necessary. One has to discard the populations of the particle unstable states in the given nucleus and (this is much harder) one has to add contributions from the decay of higher mass particle unstable states. Detailed calculations of this nature are currently in progress [27], for a small selected set of isotopes. Here, we ignore this complication and assume that the yields obtained can be used for determining general characteristics.

It is obvious that there is no power law at any temperature. (This was also found in the preceding work involving

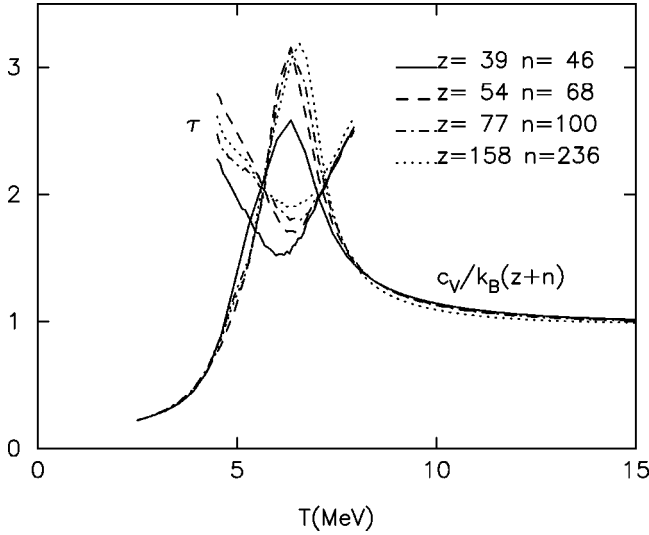


FIG. 8. Specific heat per nucleon and τ for the same model as in Fig. 7.

one-component systems [17].) Nonetheless we extract an effective value of τ by equating $\sum_{j=3}^{20} j Y_{\text{cal}}(j) / \sum_{j=3}^{20} Y_{\text{cal}}(j) = \sum_{j=3}^{20} j j^{-\tau} / \sum_{j=3}^{20} j^{-\tau}$ (plotted in Fig. 8). As a function of temperature a clear minimum in the extracted value of τ is seen. The minimum of τ can be below 2. This is not possible in the lattice gas and percolation models where a true power law emerges. We also see that the minimum of τ is achieved at least approximately at the same temperature as the maximum in specific heat (Fig. 8). Also the specific heat per particle is approximately the same whether the system consists of 100 particles or say, 300 particles. This means that the caloric curves (plots of T against E^*/A), should be roughly independent of the size of the target-projectile combination. This is shown in Fig. 9

It is also interesting to compute specific heat against temperature without including the Coulomb interaction between different clusters as done in the Wigner-Seitz approximation. The Coulomb self-energy is still present as this is part of the

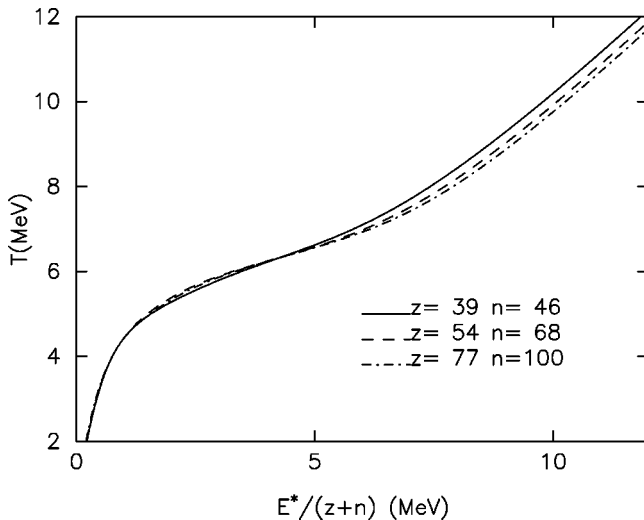


FIG. 9. Caloric curves for the same model as in Fig. 7.

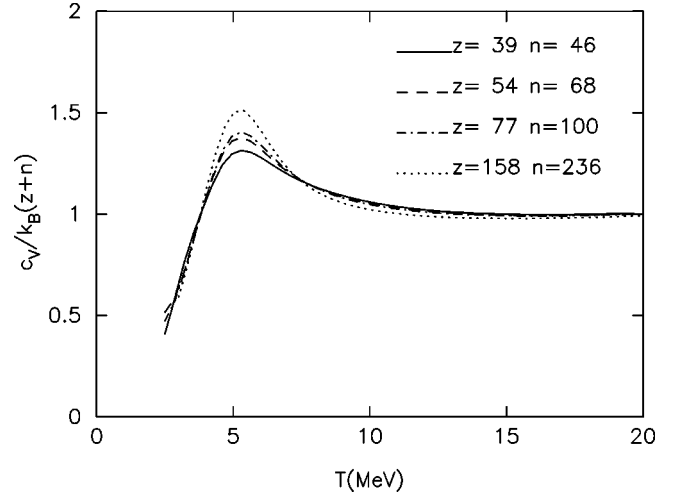


FIG. 10. Specific heat per nucleon when clusters have experimental binding energy (hence Coulomb self-energy). Coulomb interaction between the clusters is ignored.

binding energy of a nucleus. The peaks in the specific heat remain but they are reduced in height (Fig. 10).

IX. SUMMARY AND DISCUSSION

We have used a two-component soluble statistical model to investigate a few properties of nuclear systems at finite temperature and larger than normal nuclear volume such as may be applicable to the disintegration of a nuclear system formed in intermediate energy heavy ion collisions. In the last section we used experimental binding energies as input data in the model and excited states were included in the formalism using a modified Fermi-gas formula. Depending upon the particular feature that is being investigated, different inputs may be used. For example one might want to include some excited states from data tables and some from a closed expression such as used here. The model is easy and versatile enough to allow such changes with little extra work and computation.

We have, in particular, investigated the caloric curve and find that a peak in the specific heat is indeed found and at about the right temperature as suggested by experiments. We have looked at examples of isotope distributions at different temperatures. While admitting that this distribution will change as particle unstable states will decay we find that the “primary” distribution does not obey a power law at any temperature. This may be a shortcoming of the model as applied to heavy ion collisions.

The Coulomb interaction changes the specific heat in a significant way. It brings down the peak in specific heat to lower temperature. It also makes the caloric curve much more independent of the size of the system than when the Coulomb interaction was absent. However, there are some features in Fig. 8 which do not agree with experiment. The effective τ has a minimum as a function of beam energy [23] for medium size systems; however, for very large systems (central collisions of Au on Au) the minimum disappears [25]. In Fig. 8 we see the minimum remains whether the

system is of intermediate size or very large size.

This apparent contradiction with experiment can be removed by allowing more flexibility in the two-component model. In plotting Fig. 8 we assumed that the freeze-out density is independent of the size of the system. Now the Wigner-Seitz correction depends on the freeze-out density. If the freeze-out density is very low then the Wigner-Seitz correction term is small. The only Coulomb interaction that a cluster has is its own self-interaction. In this limit the minimum of τ disappears even for a medium size system. If the freeze-out density becomes lower as the system size gets bigger, one can have the situation where a minimum in τ is achieved for medium size systems but disappears for a large system. This could result from the fact that big systems require larger volume (per nucleon) to equilibrate because of much stronger long range Coulomb field.

The disappearance of the minimum in τ was studied in detail in a hybrid model [24,22]. The calculation there used a lattice gas model followed by classical molecular dynamics. The lattice gas model is used to generate the initial positions of the nucleons in the presence of nearest neighbor interaction and the Coulomb interaction. The nucleons are ascribed momenta from a Maxwell-Boltzmann distribution. They now propagate according to classical molecular dynamics in the presence of a short range and the Coulomb interactions. At asymptotic times one can clearly recognize clusters. For the smallest system $z=39$, $n=46$, the Coulomb interaction

made no significant difference. A minimum in τ as a function of temperature was found and it was close to the value predicted by a lattice gas model where Coulomb effect is totally ignored. For $z=79$, $n=118$ the minimum in τ is still present but its value is lower than 2 and it is obtained at a much lower temperature (about 2 MeV). For $z=158$, $n=236$ the minimum in τ disappears. These predictions are in agreement with experiments [23,25]. It may be possible in this type of hybrid model to investigate if for a larger system the effective freeze-out density is lower. This will be attempted in the future.

In summary, the methodology exemplified in this paper will allow quick computations of many observables seen in intermediate energy heavy ion collisions. The calculations give what is predicted by statistical models which have long standing applications in nuclear physics. The calculations are actually easier to implement than grand canonical calculations which were done for Bevalac physics (for a summary of such calculations see Ref. [26]).

ACKNOWLEDGMENTS

This research was supported in part by the U.S. Department of Energy, Grant No. DE FG02-96ER 40987, and by the Natural Sciences and Engineering Research Council of Canada.

-
- [1] P. Kreuz *et al.*, Nucl. Phys. **A556**, 672 (1993).
 - [2] J. A. Hauger *et al.*, Phys. Rev. Lett. **77**, 235 (1996).
 - [3] J. Pochodzalla *et al.*, ALADIN Collaboration, Phys. Rev. Lett. **75**, 1040 (1995).
 - [4] S. Wang *et al.*, EOS Collaboration, Phys. Rev. Lett. **74**, 2646 (1995).
 - [5] M. L. Gilkes *et al.*, EOS Collaboration, Phys. Rev. Lett. **73**, 1590 (1994).
 - [6] J. P. Bondorf, A. S. Botvina, A. S. Iljinov, I. N. Mishustin, and K. Sneppen, Phys. Rep. **257**, 133 (1995).
 - [7] D. H. E. Gross and P. A. Hervieux, Z. Phys. D **35**, 27 (1995).
 - [8] J. Pan and S. Das Gupta, Phys. Rev. C **51**, 1384 (1995).
 - [9] L. Sobotka and L. Moretto, Phys. Rev. C **31**, 668 (1985).
 - [10] J. Randrup and S. E. Koonin, Nucl. Phys. **A356**, 223 (1981).
 - [11] X. Campi and H. Krivine, Nucl. Phys. **A545**, 161c (1992).
 - [12] A. Z. Mekjian, Phys. Rev. Lett. **64**, 2125 (1990).
 - [13] H. Müller and B. D. Serot, Phys. Rev. C **52**, 2072 (1995).
 - [14] N. K. Glendenning, Phys. Rev. D **46**, 1274 (1992).
 - [15] G. E. Andrews, *Theory of Partitions*, Vol. 2 of *Encyclopedia of Mathematics and Its Applications* (Addison-Wesley, Reading, MA, 1976).
 - [16] K. C. Chase and A. Z. Mekjian, Phys. Rev. C **50**, 2078 (1994).
 - [17] S. Das Gupta and A. Z. Mekjian, Phys. Rev. C **57**, 1361 (1998).
 - [18] A. Majumder and S. Das Gupta, Phys. Rev. C **59**, 845 (1999).
 - [19] S. E. Koonin and J. Randrup, Nucl. Phys. **A474**, 173 (1987).
 - [20] D. Hahn and H. Stöcker, Nucl. Phys. **A452**, 723 (1986).
 - [21] G. Audi and A. H. Wapstra, Nucl. Phys. **A595**, 409 (1995).
 - [22] J. Pan and S. Das Gupta, Phys. Rev. C **57**, 1839 (1998).
 - [23] T. Li *et al.*, Phys. Rev. Lett. **70**, 1924 (1993).
 - [24] S. Das Gupta and J. Pan, Phys. Rev. C **53**, 1319 (1996).
 - [25] M. D'Agostino *et al.*, Phys. Rev. Lett. **75**, 4373 (1995).
 - [26] S. Das Gupta and A. Z. Mekjian, Phys. Rep. **72**, 131 (1981).
 - [27] A. Majumder (unpublished).
 - [28] S. Das Gupta, A. Majumder, S. Pratt, and A. Z. Mekjian (unpublished).
 - [29] J. Aichelin, Phys. Rep. **202**, 233 (1991).